Biochimica et Biophysica Acta, 649 (1981) 661–679
Elsevier/North-Holland Biomedical Press

BBA 79495

LACTOSE-H^+($^-$OH) TRANSPORT SYSTEM OF *ESCHERICHIA COLI*

MULTISTATE GATED PORE MODEL BASED ON HALF-SITES STOICHIOMETRY FOR HIGH-AFFINITY SUBSTRATE BINDING IN A SYMMETRICAL DIMER

FRANK J. LOMBARDI *

Laboratory of Nuclear Medicine and Radiation Biology, 900 Veteran Avenue, Los Angeles, CA 90024 (U.S.A.)

(Received April 6th, 1981)
(Revised manuscript received August 10th, 1981)

Key words: Galactoside-H^+(OH^-); Gated pore model; Half-site stoichiometry; Substrate binding; Lactose transport; (E. coli)

A model is proposed for the D-galactoside-H^+($^-$OH) transporter of *Escherichia coli* that accounts for essentially all the experimental observations established for this system to date. In this model, the functional unit is postulated to be a dimer (consisting of two copies of *lac*Y-specified polypeptide) which spans the membrane with a 2-fold symmetry axis in the membrane plane (Lancaster, J.R. (1978) J. Theor. Biol. 75, 35–50). The functional dimer is assumed to possess a single pore flanked by an inner gate (g_i) and an outer gate (g_o) and encompassing two oppositely oriented galactoside binding sites, designated m and μ. When g_o is open and g_i is closed under non-energized conditions, binding site m adopts a configuration defined as State A (i.e., m_o^A) exhibiting high affinity toward Class G^a galactosides (thiodigalactoside, melibiose, α-*p*-nitrophenylgalactoside) but low affinity for Class G^b galactosides (lactose, β-*o*-nitrophenylgalactoside, β-isopropylthiogalactoside), whereas binding site μ adopts State B (i.e., μ_o^B) displaying relatively high affinity toward Class G^b galactosides but comparatively low affinity for Class G^a galactosides; further, each $m_o^A : \mu_o^B$ dimer contains one thiol group whose reaction with *N*-ethylmaleimide inactivates the transporter unless blocked by galactoside binding at site m_o^A, while the second homologous thiol of the dimer is unreactive toward thiol reagents. Translocation of the $m_o^A : \mu_o^B$ dimer involves closing of g_o followed by opening of g_i, and causes the two thiols (as well as sites m and μ) to interchange roles in a symmetrical fashion: $m_o^A : \mu_o^B \leftrightarrow m_i^B : \mu_i^A$. In the presence of a substantial (negative) transmembrane $\Delta\tilde{\mu}_{H^+}$, the m : μ dimer is postulated to undergo an electrogenic protein conformational change to a second form, *(m : μ), in which both sites m and μ possess low affinity toward internal Class G^b substrates; galactoside transport in both m : μ and *(m : μ) is assumed to be coupled to H^+-symport ($^-$OH-antiport) with a stoichiometry of approximately 1 : 1. Finally, five characteristic predictions of the half-sites model are outlined for further tests of its validity.

Since its discovery in 1955 [1,2], the lactose transport system of *Escherichia coli* has been studied intensively (reviewed in Refs. 3–6) and has served as a paradigm for bacterial secondary active uptake sys-

* Present address: NTK Research Institute, 602 E. Elk Avenue, Glendale, CA 91205, U.S.A.

Abbreviations: β-ONPG, *o*-nitrophenyl β-D-galactopyranoside; thiodigalactoside, β-D-galactopyranosyl 1-thio-β-D-galactopyranoside; α-PNPG, *p*-nitrophenyl α-D-galactopyranoside; melibiose, 6-*O*-(α-D-galactopyranosyl)-D-glucose; lactose, 4-*O*-(β-D-galactopyranosyl)-D-glucose; allolactose, 6-*O*-(β-D-galactopyranosyl)-D-glucose; galactobiose, 6-*O*-(β-D-galactopyranosyl)-D-galactose; IPTG, isopropyl 1-thio-β-D-galactopyranoside; TMG, methyl 1-thio-β-D-galactopyranoside; Dns-(dansyl-), 5-dimethylaminonaphthalene-1-sulfonyl-; Dns^2-S-Gal, 2′-(*N*-dansyl)aminoethyl 1-thio-β-D-galactopyranoside; Dns^6-S-Gal, 6′-(*N*-dansyl)aminohexyl 1-thio-β-D-galactopyranoside; APG_0, 2-nitro-4-azidophenyl 1-thio-β-D-galactopyranoside. APG_2, 2′-*N*-(2-nitro-4-azidophenyl)aminoethyl 1-thio-β-D-galactopyranoside; CCCP, carbonyl cyanide *m*-chlorophenylhydrazone.

0005-2736/81/0000–0000/$02.50 © 1981 Elsevier/North-Holland Biomedical Press

tems [6] following verification of Mitchell's hypothesis [7] that the system functions as a galactoside-H^+ symporter (or -$^-$OH antiporter) [8–13]. On the structural level, a membrane protein required for β-galactoside transport (M protein) was identified by Fox and Kennedy [14] by means of a specific labeling procedure using radioactively labeled *N*-ethylmaleimide. Subsequent work showed that the M protein is a product of the Y-gene of the *lac* operon [15] and exhibits a molecular weight of approximately 31 000 when examined by sodium dodecyl sulfate-polyacrylamide gel electrophoresis without prior boiling in detergent [16]. On the other hand, the recently determined *lac*Y DNA sequence [17] specifies a single polypeptide of molecular weight 46 500, and Villarejo [18] has presented evidence for two *lac*Y-derived polypeptides, of molecular weights 33 000 and 15 000, in samples boiled in the presence of sodium dodecyl sulfate. These results indicate that the electrophoretic behavior of incompletely denatured M protein in sodium dodecyl sulfate is anomalous and, provided the 33- and 15-kdalton species are present prior to heating in detergent, suggest possible post-translational cleavage of some or all of the 46.5 kdalton polypeptide chains. Ehring et al. [19] have recently shown that integration of *lac*Y-determined protein into the cytoplasmic membrane occurs without proteolytic removal of a hydrophobic N-terminal peptide [20].

In 1966 Winkler and Wilson [21] showed that the affinity ($1/K_m$) of the galactoside transporter for lactose or β-ONPG uptake via facilitated diffusion in energy-poisoned cells was similar to that observed for concentrative uptake by fully energized cells. Moreover, the apparent maximum velocities for galactoside efflux and uptake (via exchange) were not markedly different in the energypoisoned cultures as compared to controls [21]. In contrast, the affinity for intracellular lactose was 100-fold lower in the actively metabolizing culture than in energy-poisoned cells, the latter displaying an affinity indistinguishable from that observed for external lactose. Winkler and Wilson concluded that the primary effect of energy-coupling on the uptake system is to lower its affinity for intracellular galactoside [21]. These results and conclusions were confirmed for the most part by Lancaster et al. [22] and are consistent with the recent demonstrations that the transport system is functionally symmetrical within the membrane under non-energized conditions [23–25].

The model of Winkler and Wilson, in conjunction with the H^+-symport/$^-$OH antiport concept of Mitchell [7] as developed by West [8] and Harold [4,26], provides for transport of the type I galactosides [3] lactose, β-ONPG, IPTG and TMG in terms of $\Delta\tilde{\mu}_{H^+}$-dependent modulation of a single galactoside binding site, where $\Delta\tilde{\mu}_{H^+}$ is the transmembrane electrochemical potential gradient of protons. As shown by Kennedy et al. [14–16,27], however, the system also displays evidence under non-energized conditions for a site possessing high affinity toward substrates designated type II galactosides (including thiodigalactoside and the α-galactosides α-PNPG [28] and melibiose) which confer protection against inactivation of the system by thiol reagents [29]. Moreover, the type I galactosides lactose and β-ONPG at 5 mM concentration do not protect against *N*-ethylmaleimide inactivation under non-energized conditions [15] and fail to reverse the protection afforded by type II galactosides [3] even though the Michaelis constants determined for lactose and β-ONPG uptake in energy-poisoned cells are on the order of 1 mM [11,21]. On the other hand, much higher concentrations of lactose (>0.1 M) are effective in protecting the transporter against *N*-ethylmaleimide inactivation in non-energized preparations [30]. These observations suggest the presence of two distinct binding sites exhibiting widely different affinities toward the various galactosides. However, genetic studies have shown that loss of lactose transport in mutants is invariably accompanied by loss of *lac*Y-dependent melibiose uptake [31] and vice versa [32], indicating that there is only one *lac*Y-determined galactoside binding site.

Several models attempting to reconcile these observations have been put forward in recent years, each based in one way or another on a $\Delta\tilde{\mu}_{H^+}$-induced change in the binding and/or translocation properties of the porter, where

$$\Delta\tilde{\mu}_{H^+} = \Delta\psi - 2.3(RT/F)\,\Delta pH = \Delta\psi - Z\,\Delta pH \qquad (1)$$

in which $\Delta\psi$ is the transmembrane electrical potential difference (interior minus exterior), ΔpH is the transmembrane pH gradient (Internal pH (pH_i) minus external pH (pH_o)), R is the gas constant, T the abso-

lute temperature, F the Faraday, and Z is 59 mV at 25°C. Thus, in a series of models from Kaback's laboratory, the transporter is proposed to exist in two asymmetric forms which undergo facile interconversion by way of electrogenic translocation reactions [33], rate-determining protonation-deprotonation [34,35], or electrogenic subunit oligomerization [36]. However, these models are not compatible with the demonstrated symmetry of the system under energy-uncoupled conditions [23–25], nor with the observations that lactose at concentrations below 5 mM does not competitively inhibit melibiose or α-PNPG binding in non-energized preparations [3,30] but is nevertheless bound and transported under these conditions [35].

A second type of model proposed by Wright et al. [30] envisions a symmetrical carrier with a single binding site exhibiting high affinity for type II galactosides but low affinity for lactose under non-energized conditions. In the presence of a substantial $\Delta\tilde{\mu}_{H^+}$, the model postulates the equivalent of a $\Delta\tilde{\mu}_{H^+}$-dependent alteration in the binding site which causes it to acquire high affinity for lactose in addition to type II galactosides. Although the concept of a $\Delta\tilde{\mu}_{H^+}$-induced change in binding specificity is a useful one (see below), the model of Wright et al. does not account for high-affinity uptake of lactose or β-ONPG under non-energized conditions, as demonstrated convincingly by Winkler and Wilson [21], Cecchini and Koch [11], and Lancaster and Hinkle [24,25].

A third model proposed by Lancaster [37] embodies an important conceptual advance in postulating that the transport system functions as a dimer composed of two identical protomers symmetrically disposed within the membrane. The model is consistent with the modern gated pore concept of active transport [38] and incorporates the key experimental finding by Lancaster and Hinkle [25] that the type II galactoside α-PNPG at a concentration (0.3 mM) greatly exceeding its affinity for the transporter as judged by its ability to protect against *N*-ethylmaleimide inactivation [27] nevertheless fails to inhibit the facilitated diffusion of lactose in inverted vesicles. However, Lancaster's model does not provide for high-affinity binding of type II galactosides under non-energized conditions [27].

It is the purpose of this report to show that essentially all the binding, transport and genetic properties established to date for the *E. coli* galactoside transporter are readily interpretable in terms of a new model that combines and extends the concepts of Winkler and Wilson [21], Lancaster [37] and Wright et al. [30]. This model derives from the addition of three supplementary concepts to those described above. First, studies on the human erythrocyte hexose transporter [39,40] support the notion that a single asymmetrically disposed binding site located between the inner gate (g_i) and the outer gate (g_o) of a pore may exhibit a different binding specificity when exposed to the internal compartment (g_i open, g_o closed) than when facing the exterior (g_i closed, g_o open) by virtue of differing interactions of various moieties in the bound substrate with the transporter in the two configurations of the pore. Second, placing two equivalent asymmetric binding sites in opposing orientations between the inner and outer gates of a single pore formed by the symmetrical dimer of Lancaster [37] provides a simple solution to the riddle of the two binding sites for the *E. coli* galactoside transporter, and is equivalent in this system to half-of-the-sites stoichiometry for high-affinity substrate binding. Third, the results of Winkler and Wilson [21] and Wright et al. [30] on the effect of imposing a large asymmetric $\Delta\tilde{\mu}_{H^+}$ on this inherently symmetrical system are rationalized by postulating a major $\Delta\tilde{\mu}_{H^+}$-induced change in binding specificity in one or both of the binding sites, analogous in some respects to voltage regulation of transport activity in the action potential Na^+ channel of nerve cell membranes [41]. A preliminary report of some of these concepts was presented previously [42].

Observational requirements to be satisfied by models for the galactoside transporter

To facilitate comparison of the half-sites model with known characteristics of the transport system, the major experimentally established properties of the transporter are collected and numbered below. In the following, the earlier classification of various galactosides into type I and type II substrates by Kennedy and coworkers [16] is retained in principle, but the groupings are renamed and extended in accordance with more recent findings to embrace three Classes of galactosides as follows:

Class G^a substrates (equivalent to Kennedy's type II galactosides), including thiodigalactoside, various dansylated galactosides [33], and the α-galactosides melibiose and α-PNPG;

Class G^b substrates (equivalent to Kennedy's type I galactosides), including the β-galactosides lactose, β-ONPG, TMG and IPTG;

Class G^c substrates, including the azido-galactosides APG_0 and APG_2 [43,44].

Ob. 1. The properties of the transport system in inverted membrane vesicles are essentially indistinguishable from those observed in vesicles of native orientation when $\Delta\psi = \Delta pH = 0$, or in response to artificially imposed $\Delta\tilde{\mu}_{H^+}$'s, showing that the transporter is functionally symmetrical within the membrane [23–25].

Ob. 2. Genetic evidence suggests that:

(a) the galactoside transporter specified by the *lac*Y gene functions without the direct participation of any other protein [17];

(b) there is most probably only one galactoside binding site specified by the *lac*Y gene [31].

Ob. 3. Under non-energized conditions two types of *lac*Y-determined binding sites are demonstrable:

(a) a site which mediates high-affinity binding [27,30,33,45–47] and translocation [45] of Class G^a galactosides, leading to protection of the transport system against inactivation by thiol reagents, but which exhibits only low affinity for Class G^b or Class G^c galactosides [27,29,30,43,45];

(b) a site that catalyzes facilitated diffusion of the Class G^b galactosides lactose and β-ONPG with moderately high affinity [21,11] and with a measured galactoside-H^+ stoichiometry near 1 : 1 [9,48], but which is not inhibited by the Class G^a galactosides α-PNPG and Dns^6S-Gal at comparatively high concentrations [24,25];

(c) moreover, when $\Delta\psi = \Delta pH = 0$, the transporter mediates a very rapid exchange diffusion of lactose [34,35] under conditions in which lactose is present at high concentrations (≥10 mM) on both sides of the membrane.

Ob. 4. In highly energized cells or vesicles bearing a large (negative) $\Delta\tilde{\mu}_{H^+}$, the transporter exhibits profoundly different properties from those observed when $\Delta\psi = \Delta pH = 0$, as reflected by changes in both the kinetics and substrate specificity of galactoside transport listed below.

(a) The apparent affinity for internal lactose is reduced 100-fold or more [21,22,49].

(b) The maximum velocity of lactose uptake appears to increase somewhat [21], and there is a small or modest increase in the affinity for external lactose [30,35,36].

(c) Uptake of thiodigalactoside [21] and α-PNPG [45,50] is now subject to competitive inhibition by low concentrations of lactose and other Class G^b galactosides [45], and comparatively low levels of lactose now protect against *N*-ethylmaleimide inactivation [51].

(d) Lactose uptake is subject to competitive inhibition by low concentrations of the Class G^a galactosides α-PNPG [45,52] and Dns^6S-Gal [33] in energized cells or vesicles.

(e) Exchange diffusion of lactose now proceeds at the same rate as net lactose uptake or efflux [21,22], and is slower than the low-affinity exchange observed when $\Delta\psi = \Delta pH = 0$.

(f) The maximum velocity of uptake observed under energized conditions varies markedly from galactoside to galactoside [29].

(g) In the presence of a substantial $\Delta\tilde{\mu}_{H^+}$, low concentrations of α-PNPG [53] and of the azido-galactosides APG_0 and APG_2 [43,44] competitively inhibit lactose uptake and are able to cause specific photoinactivation of the transport system; under non-energized conditions, specific photoinactivation has been observed with α-PNPG [53] but not with APG_0 or APG_2 [43,44].

(h) The experimentally determined galactoside-H^+/$^-$OH transport stoichiometry in energized cells is near 1.0 [12], but steady-state accumulation levels of lactose are always somewhat lower than predicted on the assumption of thermodynamic equilibrium between $\Delta\mu_{lac}$ and $\Delta\tilde{\mu}_{H^+}$ with 1 : 1 stoichiometry [54,55], indicating the existence of low-affinity [21,22] galactoside 'leak' pathway(s) in which galactoside translocation is not coupled to H^+-symport/$^-$OH-antiport; since efflux of lactose from preloaded cells is blocked nearly completely by thiol reagents [51,56], the lactose leak is probably mediated by the galactoside transporter itself.

Finally, among the results to be accounted for by models of the transporter are the measured binding and transport affinities (half-saturation concentrations) of the system toward various substrates under

both non-energized and highly energized conditions. In view of the evidence indicating only a single genetically determined galactoside binding site (Ob. 2b), the Observations outlined above suggest that this site exists in at least four distinct states, as follows:

State A, defined as that state of the binding site occurring in non-energized preparations in which Class G[a] galactosides are preferentially bound;

State B, defined as that state of the binding site occurring in non-energized preparations in which

TABLE I

EXPERIMENTALLY MEASURED AFFINITY OF THE *E. COLI* GALACTOSIDE TRANSPORTER FOR VARIOUS GALACTOSIDES

Half-saturation constants determined from binding (K_D), transport (K_T) or competitive inhibition (K_I) experiments. For definitions of the State symbols (A, B, C, D, E, F), see the text.

Galactoside class	Galactoside	K_D, K_T, *or* K_I (mM) measured in							
		Non-energized preprations				Energized preparations			
		State A		State B		State C (or E)		State D (or F)	
		Value	Ref.	Value	Ref.	Value	Ref.	Value	Ref.
G [a]	α-PNPG	0.007	(27) [a]	>>0.3	(25) [f]	0.006	(52) [m]	>0.3	(52) [p]
		0.009	(52) [b]			0.004	(47) [m]		
		0.021	(45) [c]						
		0.021	(47) [b]						
	thiodigalactoside	0.067	(27) [a]	~0.7	(24) [g]	0.040	(30) [n]		
		0.048	(46) [b]						
		0.055	(30) [c]						
	Dns^2-S-Gal	0.030	(45) [c]	>>0.3 [h]	(25) [f]	0.035	(30) [n]		
G [b]	Lactose	>>5	(61) [d]	0.9	(21) [i]	0.26	(22) [o]	16	(21) [o]
		18	(30) [c]	0.95	(24) [j]	0.20	(62) [n]	25	(49) [q]
		18.9	(35) [e]	1.2	(35) [k]	0.05	(30) [n]	∞	(22) [o]
	β-ONPG	>>5	(61) [d]	1.0	(11) [l]	0.5	(21) [o]	>20	(21) [o]
G [c]	APG_0	–		–		0.075	(43) [n]	–	

[a] K_D determined in sonicated membranes from strain K12 A-3245.
[b] K_D in membrane vesicles from strain ML308-225.
[c] K_D measured with cytoplasmic membranes of strain T31RT [45] or strain T185 [30].
[d] Based on failure of 5 mM sugar to protect against *N*-ethylmaleimide in ML308-225 ($\Delta\tilde{\mu}_{H^+} = 0$).
[e] K_T for facilitated diffusion in CCCP-treated ML308-225 membrane vesicles.
[f] Based on failure of 0.3 mM galactoside to inhibit facilitated diffusion of lactose in inverted vesicles from strain ML308-225.
[g] Calculated from data [24] showing that 17 mM thiodigalactoside produced 81% inhibition in the initial rate of 4.7 mM lactose uptake via facilitated diffusion in inverted vesicles from strain ML308-225, assuming competitive inhibition.
[h] Based on observations with Dns^6-S-Gal [25].
[i] K_T determined in ML308-225 cells poisoned with azide + iodoacetate.
[j] K_T for facilitated diffusion in inverted vesicles from strain ML308-225.
[k] K_T for efflux ($\Delta\psi = \Delta pH = 0$) in K^+-valinomycin-equilibrated ML308-225 vesicles.
[l] K_T for facilitated diffusion in CCCP-treated cells of strain ML308.
[m] K_I for inhibition of D-lactate-stimulated lactose uptake in ML308-225 vesicles.
[n] K_T for D-lactate-stimulated uptake in ML308-225 membrane vesicles.
[o] K_T determined in respiring cells of strain ML308-225.
[p] Based on the ability of >0.3 mM α-PNPG to inhibit dilution-induced efflux of 4 mM intravesicular lactose from ML308-225 membrane vesicles.
[q] K_T for temperature-induced efflux from ML308-225 membrane vesicles in the presence of D-lactate.

Class G^b galactosides are preferentially bound;

State C (or E), defined as that state of the binding site existing in highly energized preparations in which galactosides of Classes G^a, G^b and G^c are bound with high apparent affinity;

State D (or F), defined as a form of the binding site occurring under highly energized conditions which exhibits comparatively low affinity for all galactosides.

Table I presents a compilation from the literature of the experimentally determined affinities manifested by the transport system toward various galactosides under both non-energized and highly energized conditions. The values quoted in Table I are functions of external pH (pH_o), internal pH (pH_i) and $\Delta\psi$, and for the non-energized preparations were determined in the range $pH_o = pH_i \simeq 6.5–7.0$ ($\Delta\psi = 0$); for the columns representing energized preparations the values given are for $\Delta\psi \simeq -85$ to -145 mV or more [57], $pH_i \simeq 7.8$ [48,58–60], and pH_o in the range pH 6.5–7.5.

Half-sites model for the *E. coli* galactoside transporter

The properties of the transporter are simpler and more clearly defined experimentally for circumstances in which $\Delta\psi = \Delta pH = 0$. Accordingly, the half-sites model is described first for these non-energized conditions. Extension to systems bearing a substantial transmembrane $\Delta\tilde{\mu}_{H^+}$ is discussed in a later section.

Postulates of the model (for $\Delta\psi = \Delta pH = 0$)

Po. 1. The functional unit in the *E. coli* galactoside transporter is proposed to be a dimer containing two copies of *lac*Y-specified polypeptide which spans the membrane and possesses a 2-fold symmetry axis within the plane of the membrane [37].

Po. 2a. The functional dimer is assumed to possess a single pore containing two galactoside binding sites (designated m and μ) which are oriented with opposite polarities, the dimer being represented by the notation m : μ in biological membranes of native orientation or in reconstituted systems [63] and by μ : m in biological membranes of inverted orientation [64].

Po. 2b. The portion of the pore containing the two binding sites in the m : μ dimer is flanked by an outer gate (g_o) and an inner gate (g_i).

Po. 3. In the m : μ dimer under non-energized conditions with g_o open and g_i closed, binding site m is in State A (i.e., m_o^A) and exhibits high affinity for Class G^a galactosides but only low affinity toward Class G^b or G^c galactosides (as defined above) while binding site μ is in State B (i.e., μ_o^B) and manifests relatively high affinity toward Class G^b galactosides but comparatively low affinity for Class G^a and G^c galactosides (Table I). Similarly, when g_o is closed and g_i is open in the m : μ dimer, binding site m assumes State B (i.e., m_i^B) and binding site μ adopts State A (i.e., μ_i^A). Accordingly, translocation of the (unoccupied) binding sites may be written

$$m_o^A : \mu_o^B \rightleftharpoons m_i^B : \mu_i^A \tag{2}$$

in which both orientations of the m : μ dimer exhibit half-of-the-sites stoichiometry for high-affinity substrate binding with either a Class G^a or Class G^b galactoside.

Po. 4. Associated with each of the galactoside binding sites within the pore is presumed to be a subsite, represented in the case of an H^+-symporting mechanism by the symbolic notation -X, whose protonation is markedly enhanced by binding of a galactoside at the associated primary site. Translocation in the m : μ dimer normally occurs when a galactoside binding site is either (i) unoccupied and its associated -X group unprotonated, or (ii) occupied and its associated subsite protonated, $-X \cdot H^+$, i.e.,

$$m_o^A[-X \quad : \quad X-]\,\mu_o^B \rightleftharpoons m^{\dagger}[-X \quad : \quad X-]\,\mu^{\dagger} \rightleftharpoons m_i^B[-X \quad : \quad X-]\,\mu_i^A \tag{3}$$

$$m_o^A[XH^+, G : \quad X-]\,\mu_o^B \rightleftharpoons m^{\ddagger}[XH^+, G : \quad X-]\,\mu^{\ddagger} \rightleftharpoons m_i^B[XH^+, G : \quad X-]\,\mu_i^A \tag{4}$$

$$m_o^A[-X \quad : G, {}^+HX]\,\mu_o^B \rightleftharpoons m^{\dagger}[-X \quad : G, {}^+HX]\,\mu^{\ddagger} \rightleftharpoons m_i^B[-X \quad : G, {}^+HX]\,\mu_i^A \tag{5}$$

$$m_o^A[XH^+, G : G, {}^+HX]\,\mu_o^B \rightleftharpoons m^{\ddagger}[XH^+, G : G, {}^+HX]\,\mu^{\ddagger} \rightleftharpoons m_i^B[XH^+, G : G, {}^+HX]\,\mu_i^A \tag{6}$$

where G denotes a galactoside molecule, [ ] represents the pore within the m : μ dimer, upper and lower horizontal bars depict the inner gate (g_i) and the outer gate (g_o) respectively, and the superscripts † and ‡ denote the transition states for translocation in which both inner and outer gates are in the closed configuration. (Alternatively, for an $^{-}$OH-antiporting mechanism, each galactoside binding site would be associated with an $^{-}$OH-binding subsite in which binding of $^{-}$OH would be markedly impeded by galactoside binding at the associated primary site.) In order to prevent the transporter from acting as a proton- (or $^{-}$OH-) conducting uncoupler in the absence of bound galactoside, it is assumed that protonation of group -X (or, alternatively, dissociation of $^{-}$OH) within a subsite blocks formation of the transition state for translocation (indicated by ‡) unless a compensating change is brought about by binding of a galactoside to the associated galactoside binding site (indicated by ‡). The translocations in Eqns. 3–6 (reading from left to right) are accompanied by the effective inward translocation of $N_{0,0}$, $N_{1,0}$, $N_{0,1}$, and $N_{1,1}$ positive charges, respectively, where in accordance with Mitchell's proton-well concept [65] the various N values are not necessarily integers [66] since the m : μ dimer would presumably bear charged groups and electric dipoles in addition to -XH^+ which would undergo net transmembrane displacements as a result of translocation. The data of Kaczorowski and Kaback [34] suggest the following qualitative predictions for the various N values:

$$N_{1,1} \simeq 0 \text{ (Ref. 34)} \tag{7a}$$

$$N_{1,0} \simeq N_{0,1} < 0 \text{ (Ref. 34)} \tag{7b}$$

$$N_{0,0} \simeq N_{1,0} + N_{0,1} << 0 \tag{7c}$$

Po. 5. Associated with each functional dimer is a single thiol group whose reaction with -SH reagents causes inactivation of the transport system unless blocked by galactoside binding. The second homologous thiol group of the dimer is unreactive toward these reagents, and the two thiols are assumed to interchange roles after each translocation of the dimer. Thus, absorbing the explicit -X and -XH^+ symbolism of Eqns. 3–6 (as well as the transition state species) into the adjacent m_o^A, μ_o^B, m_i^B and μ_i^A notation, the translocation reactions may now be expressed (with H^+-symport/$^{-}$OH-antiport implicitly understood) as follows:

$$m_o^A[\underline{-SH} \quad : \quad](\underline{HS-})\,\mu_o^B \rightleftharpoons m_i^B(\underline{-SH})[\quad : \quad \underline{HS-}]\,\mu_i^A \tag{8}$$

$$m_o^A[\underline{-SH}, G : \quad](\underline{HS-})\,\mu_o^B \rightleftharpoons m_i^B(\underline{-SH})[G : \quad \underline{HS-}]\,\mu_i^A \tag{9}$$

$$m_o^A[\underline{-SH} \quad : G](\underline{HS-})\,\mu_o^B \rightleftharpoons m_i^B(\underline{-SH})[\quad : G, \underline{HS-}]\,\mu_i^A \tag{10}$$

$$m_o^A[\underline{-SH}, G : G](\underline{HS-})\,\mu_o^B \rightleftharpoons m_i^B(\underline{-SH})[G : G, \underline{HS-}]\,\mu_i^A \tag{11}$$

in which HS- or -SH denotes the reactive form of the thiol (protected by galactoside binding) and (HS-) or (-SH) represents the unreactive form of the thiol.

Kinetic Representation ($\Delta\psi = \Delta p\mathrm{H} = 0$)

Fig. 1 shows minimal schematic representations of binding and translocation posited by the half-sites model for the m : μ functional dimer in the presence of a Class G^a galactoside (Fig. 1 A) or a Class G^b galactoside (Fig. 1B) when $\Delta\psi$ and ΔpH are near zero in membrane structures of native orientation. More complex schemes involving interactions with two different galactosides of the same or different Classes may also be constructed, though the minimal schemes in Fig. 1 generally provide an adequate intuitive basis for qualitative predictions. In Fig. 1, solid and dashed branching arrows designate intrinsically high-affinity and intrinsically low-affinity binding, respectively, of the indicated galactoside together with binding of one H^+ ion (Eqns. 3–6) or dissociation of one $^{-}$OH ion, with the binding order unspecified. Each composite galactoside-H^+/$^{-}$OH step is associated with a pH-dependent microscopic dissociation constant ($K_{j,k}^o, K_{j,k}^i$, Fig. 1) given by the ratio of the composite dissociation and association rate constants for the step,

$$K_{j,k}^o = k_{j,k}^{-o}/k_{j,k}^{+o}, \quad K_{j,k}^i = k_{j,k}^{-i}/k_{j,k}^{+i} \tag{12}$$

the ratios having dimensions of galactoside concentration (mM); the effects of variation in pH on the H^+-binding/$^{-}$OH-dissociation component are absorbed into the overall pH-dependence of the constant. Pairs of vertical arrows in Fig. 1 designate translocation reactions (Eqns. 8–11) whose relative rates are indi-

A. Class G^a Galactosides (n = -1, -2, -3, . . .)

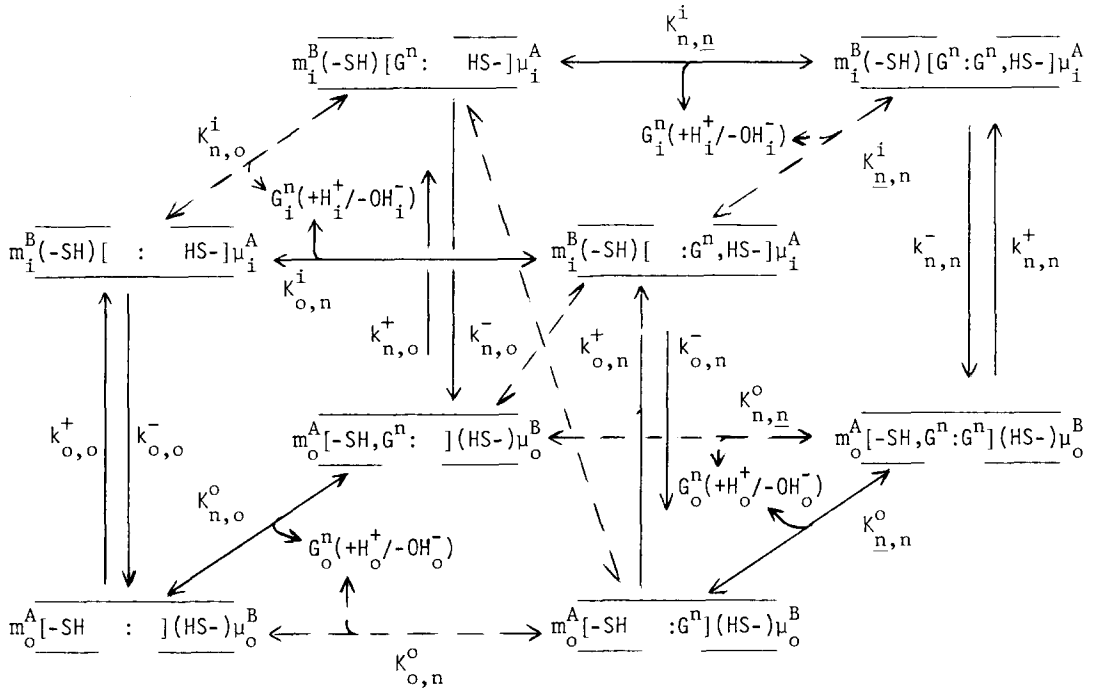

B. Class G^b Galactosides (n = +1, +2, +3, . . .)

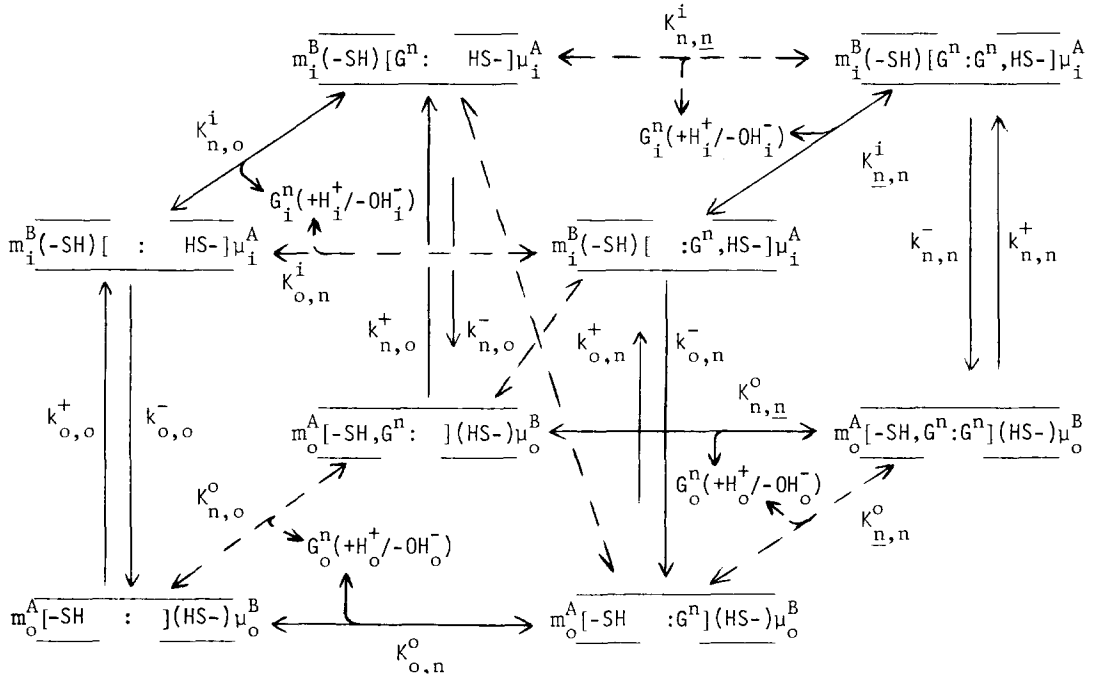

cated in a rough fashion by the lengths of the arrows. The lengths of the two opposing arrows of a pair also provide a qualitative indication of the equilibrium constant for partitioning of the species in question between inward facing (i) and outward facing (o) orientations, the equilibrium constant being given by the ratio $k^{+}_{j,k}/k^{-}_{j,k}$ (Fig. 1). The dashed diagonals with single barbs in Fig. 1 are included to suggest the possibility of trans-site migration of the sequestered galactoside(s) within the pore during translocation, but will not be considered further here.

The schemes in Fig. 1 show that the half-sites model satisfies the observational requirements for functional symmetry of the transport system (Ob. 1) and for a single genetically determined galactoside binding site (Ob. 2). Moreover, in form m : μ the site in State A binds thiodigalactoside, α-PNPG, melibiose, and dansylated galactosides with high affinity leading to protection against *N*-ethylmaleimide inactivation (Ob. 3a) whereas the binding site in State B catalyzes comparatively high-affinity facilitated diffusion of lactose or β-ONPG in a manner that is not subject to competitive inhibition by 0.3 mM α-PNPG (Ob. 3b).

A quantitative test of the half-sites model is obtainable in principle by assuming values for the microscopic rate constants in Fig. 1 and Eqn. 12, then calculating the observable transport K_m and V_{max} values and comparing with experiment. However, the calculations are nontrivial, since the full steady-state rate equations for the kinetic schemes in Fig. 1 are complicated expressions containing terms up to third order in the concentration of internal and external galactoside [67]. Approximate simplified expressions have been derived (Lombardi, F.J., unpublished data) which allow comparison of the calculated parameters with experimental values obtained for lactose transport in non-energized ML308-225 cells [21] and membrane vesicles [34,35]. Thus, assuming the following values for the microscopic constants in Fig. 1 and Eq. 12 ($G^n_o = G^1_o$ = Lactose$_o$, $G^n_i = G^1_i$ = Lactose$_i$, $\Delta\psi = \Delta pH = 0$, pH $\simeq$ 7, 23–25°C),

$$k^{+}_{0,0} = k^{-}_{0,0} \simeq 1000\ \mu\text{mol/min per g wet cells} \quad (13a)$$

$$k^{+}_{1,0} = k^{-}_{0,1} \simeq 1700\ \mu\text{mol/min per g wet cells} \quad (13b)$$

$$k^{+}_{0,1} = k^{-}_{1,0} \simeq 40\ \mu\text{mol/min per g wet cells} \quad (13c)$$

$$k^{+}_{1,1} = k^{-}_{1,1} > 400\ \mu\text{mol/min per g wet cells} \quad (13d)$$

$$K^{o}_{1,0} = \frac{k^{-o}_{1,0}}{k^{+o}_{1,0}} \simeq \frac{1700\ \mu\text{mol/min per g wet cells}}{(170\ \mu\text{mol/min per g wet cells})(\text{mM})^{-1}} \simeq \frac{k^{-i}_{0,1}}{k^{+i}_{0,1}} = K^{i}_{0,1} \simeq 10\ \text{mM} \quad (13e)$$

$$K^{o}_{0,1} = \frac{k^{-o}_{0,1}}{k^{+o}_{0,1}} \simeq \frac{20\ \mu\text{mol/min per g wet cells}}{(85\ \mu\text{mol/min per g wet cells})(\text{mM})^{-1}} \simeq \frac{k^{-i}_{1,0}}{k^{+i}_{1,0}} = K^{i}_{1,0} \simeq 0.235\ \text{mM} \quad (13f)$$

$$K^{o}_{\underline{1},1} = \frac{k^{-o}_{1,\underline{1}}}{k^{+o}_{\underline{1},1}} \simeq \frac{2000\ \mu\text{mol/min per g wet cells}}{(85\ \mu\text{mol/min per g wet cells})(\text{mM})^{-1}} \simeq \frac{k^{-i}_{1,\underline{1}}}{k^{+i}_{1,\underline{1}}} = K^{i}_{1,\underline{1}} \simeq 23.5\ \text{mM} \quad (13g)$$

Fig. 1. Kinetic representation of symmetrical binding and translocation schemes postulated by the half-sites model for the *E. coli* galactoside transporter in the presence of the nth galactoside (G^n) of Class G^a (A) or Class G^b (B) in membrane structures of native orientation when $\Delta\psi = \Delta pH = 0$. The proposed dimeric pore containing two oppositely oriented binding sites (m and μ, each binding one galactoside plus one H^+ (Eqns. 3–6) or, alternatively, one galactoside or one $^-$OH) in the m : μ functional dimer is represented by [:], while upper and lower horizontal bars designate the inner and outer gates of the pore. The subscript i or o denotes accessibility of the binding sites to galactosides and $H^+/^-OH$ in the inner or outer compartment, respectively, corresponding to an open configuration for the inner or the outer gate. Each binding site exists in State A or State B (indicated by superscripts) corresponding to preferential binding of galactosides of Class G^a or Class G^b, respectively. Solid and dashed branching arrows denote intrinsically high-affinity and intrinsically low-affinity binding, respectively, of the indicated galactoside; binding of $H^+/^-OH$ is not shown explicitly, but expresses itself kinetically through the pH-dependence of the galactoside dissociation constants, i.e., $K^o_{j,k}$ and $K^i_{j,k}$ (see text). Pairs of vertical arrows designate translocation steps and are characterized by the rate constants $k^+_{j,k}$ and $k^-_{j,k}$; dashed diagonals with single barbs suggest the possibility of trans-site migration within the pore during translocation. The thiodigalactoside-protectable thiol group is represented by -SH or HS- in the reactive configuration, and by (-SH) or (HS-) in the unreactive configuration (Eqns. 8–11).

$$K^{o}_{1,\underline{1}} = \frac{k^{-o}_{1,\underline{1}}}{k^{+o}_{1,\underline{1}}} \simeq \frac{40\ \mu\text{mol/min per g wet cells}}{(72\ \mu\text{mol/min per g wet cells})(\text{mM})^{-1}}$$

$$\simeq \frac{k^{-i}_{1,\underline{1}}}{k^{+i}_{1,\underline{1}}} = K^{i}_{1,\underline{1}} \simeq 0.56\ \text{mM} \qquad (13h)$$

which are consistent with microscopic reversibility, viz.,

$$\frac{k^{+}_{0,0}k^{-}_{0,1}K^{o}_{0,1}}{k^{-}_{0,0}k^{+}_{0,1}K^{i}_{0,1}} = \frac{k^{+}_{0,1}k^{-}_{1,1}K^{o}_{1,1}}{k^{-}_{0,1}k^{+}_{1,1}K^{i}_{1,1}} = \frac{k^{+}_{1,1}k^{-}_{1,0}K^{i}_{1,1}}{k^{-}_{1,1}k^{+}_{1,0}K^{o}_{1,1}}$$

$$= \frac{k^{+}_{1,0}k^{-}_{0,0}K^{i}_{1,0}}{k^{-}_{1,0}k^{+}_{0,0}K^{o}_{1,0}} = \left[\frac{(\text{Lactose})_i}{(\text{Lactose})_o}\right]_{eq} = K_{eq} \qquad (14)$$

(where $K_{eq} = 1$ for $\Delta\psi = \Delta\text{pH} = 0$), the high-affinity K_m, $(\gamma)_{0.5}$, and the high-affinity V_{max}, v, under zero-trans conditions are given by the approximate expressions

$$(\gamma^{o})_{0.5} \simeq \tfrac{1}{2}\{(f^{o}_{1,0}) + (f^{o}_{0,1})\} = \tfrac{1}{2}\{(f^{i}_{0,1}) + (f^{i}_{1,0})\}$$

$$\simeq (\gamma^{i})_{0.5} \simeq 0.90\ \text{mM} \qquad (15a)$$

$$v^{+} \simeq \tfrac{1}{2}(v^{+}_{1,0} + v^{+}_{0,1}) = \tfrac{1}{2}(v^{-}_{0,1} + v^{-}_{1,0})$$

$$\simeq v^{-} \simeq 19.2\ \mu\text{mol/min per g wet cells} \qquad (15b)$$

where [68]

$$(f^{o}_{1,0}) \simeq v^{+}_{1,0}\left(1 + \frac{k^{+}_{0,0}}{k^{-}_{0,0}}\right)\left[\frac{1}{k^{+}_{1,0}}\left(1 + \frac{k^{-}_{1,0}}{k^{-i}_{1,0}}\right) + \frac{1}{k^{-o}_{1,0}}\right]K^{o}_{1,0}$$

$$= v^{-}_{0,1}\left(1 + \frac{k^{-}_{0,0}}{k^{+}_{0,0}}\right)\left[\frac{1}{k^{-}_{0,1}}\left(1 + \frac{k^{+}_{0,1}}{k^{-o}_{0,1}}\right) + \frac{1}{k^{-i}_{0,1}}\right]K^{i}_{0,1}$$

$$\simeq (f^{i}_{0,1}) \simeq 0.89\ \text{mM} \qquad (16a)$$

$$(f^{o}_{0,1}) \simeq v^{+}_{0,1}\left(1 + \frac{k^{+}_{0,0}}{k^{-}_{0,0}}\right)\left[\frac{1}{k^{+}_{0,1}}\left(1 + \frac{k^{-}_{0,1}}{k^{-i}_{0,1}}\right) + \frac{1}{k^{-o}_{0,1}}\right]K^{o}_{0,1}$$

$$= v^{-}_{1,0}\left(1 + \frac{k^{-}_{0,0}}{k^{+}_{0,0}}\right)\left[\frac{1}{k^{-}_{1,0}}\left(1 + \frac{k^{+}_{1,0}}{k^{-o}_{1,0}}\right) + \frac{1}{k^{-i}_{1,0}}\right]K^{i}_{1,0}$$

$$\simeq (f^{i}_{1,0}) \simeq 0.91\ \text{mM} \qquad (16b)$$

$$\frac{1}{v^{+}_{1,0}} \simeq \frac{1}{k^{+}_{1,0}} + \frac{1}{k^{-}_{0,0}} + \frac{k^{-}_{1,0}}{k^{-i}_{1,0}}\left(\frac{1}{k^{+}_{1,0}} + \frac{1}{k^{-}_{1,0}}\right)$$

$$= \frac{1}{k^{-}_{0,1}} + \frac{1}{k^{+}_{0,0}} + \frac{k^{+}_{0,1}}{k^{-o}_{0,1}}\left(\frac{1}{k^{+}_{0,1}} + \frac{1}{k^{-}_{0,1}}\right) \simeq \frac{1}{v^{-}_{0,1}}$$

$$\simeq \frac{1}{18.9\ \mu\text{mol/min per g wet cells}} \qquad (16c)$$

$$\frac{1}{v^{+}_{0,1}} \simeq \frac{1}{k^{+}_{0,1}} + \frac{1}{k^{-}_{0,0}} + \frac{k^{-}_{0,1}}{k^{-i}_{0,1}}\left(\frac{1}{k^{+}_{0,1}} + \frac{1}{k^{-}_{0,1}}\right)$$

$$= \frac{1}{k^{-}_{1,0}} + \frac{1}{k^{+}_{0,0}} + \frac{k^{+}_{1,0}}{k^{-o}_{1,0}}\left(\frac{1}{k^{+}_{1,0}} + \frac{1}{k^{-}_{1,0}}\right) \simeq \frac{1}{v^{-}_{1,0}}$$

$$\simeq \frac{1}{19.4\ \mu\text{mol/min per g wet cells}} \qquad (16d)$$

It should be noted that although sites μ^{B}_{o} and m^{A}_{o} possess respectively high and low intrinsic affinities for lactose binding as embodied in the dissociation constants $K^{o}_{0,1}$ and $K^{o}_{1,0}$ (Fig. 1B and Eqns. 13e and 13f), lactose transport mediated by either site μ or m in the singly-occupied m : μ dimer exhibits relatively high affinity (Eqns. 16a and 16b) due to the fact that the rapid equilibrium assumption does not apply to the composite dissociations depicted by the branching arrows in Fig. 1, since such steps may well encompass rate-limiting protein isomerizations linking galactoside dissocition to H^{+}-dissociation/$^{-}$OH-binding. Similarly, the low-affinity K_m, $(\Gamma)_{0.5}$, and low-affinity V_{max}, V, predicted by Fig. 1B under zero-trans conditions are given by the approximate expressions

$$(\Gamma^{o})_{0.5} \simeq \tfrac{1}{2}\{(f^{o}_{1,\underline{1}}) + (f^{o}_{\underline{1},1})\} = \tfrac{1}{2}\{(f^{i}_{1,\underline{1}}) + (f^{i}_{\underline{1},1})\}$$

$$\simeq (\Gamma^{i})_{0.5} \simeq 17.8\ \text{mM} \qquad (17a)$$

$$V^{+} \simeq \tfrac{1}{2}(v^{+}_{\underline{1},1} + v^{+}_{1,\underline{1}}) = \tfrac{1}{2}(v^{-}_{1,\underline{1}} + v^{-}_{\underline{1},1}) \simeq V^{-}$$

$$\simeq 25.7\ \mu\text{mol/min per g wet cells} \qquad (17b)$$

where [68]

$$(f^{o}_{1,\underline{1}}) \simeq v^{+}_{1,1}\left(1 + \frac{k^{+}_{0,1}}{k^{-}_{0,1}}\right)\left[\frac{1}{k^{+}_{1,1}}\left(1 + \frac{k^{-}_{1,1}}{k^{-i}_{1,1}}\right) + \frac{1}{k^{-o}_{1,1}}\right]K^{o}_{1,1}$$

$$= v^{-}_{1,\underline{1}}\left(1+\frac{k^{-}_{1,0}}{k^{+}_{1,0}}\right)\left[\frac{1}{k^{-}_{1,1}}\left(1+\frac{k^{+}_{1,1}}{k^{-o}_{1,\underline{1}}}\right)+\frac{1}{k^{-i}_{1,\underline{1}}}\right]K^{i}_{1,\underline{1}}$$

$$\simeq (f^{i}_{1,\underline{1}}) \simeq 12.7 \text{ mM} \qquad (18a)$$

$$(f^{o}_{1,\underline{1}}) \simeq v^{+}_{1,\underline{1}}\left(1+\frac{k^{+}_{1,0}}{k^{-}_{1,0}}\right)\left[\frac{1}{k^{+}_{1,1}}\left(1+\frac{k^{-}_{1,1}}{k^{-i}_{1,\underline{1}}}\right)+\frac{1}{k^{-o}_{1,\underline{1}}}\right]K^{o}_{1,\underline{1}}$$

$$= v^{-}_{\underline{1},1}\left(1+\frac{k^{-}_{0,1}}{k^{+}_{0,1}}\right)\left[\frac{1}{k^{-}_{1,1}}\left(1+\frac{k^{+}_{1,1}}{k^{-o}_{\underline{1},1}}\right)+\frac{1}{k^{-i}_{\underline{1},1}}\right]K^{i}_{\underline{1},1}$$

$$\simeq (f^{i}_{\underline{1},1}) \simeq 22.9 \text{ mM} \qquad (18b)$$

$$\frac{1}{v^{+}_{\underline{1},1}} \simeq \frac{1}{k^{+}_{1,1}}+\frac{1}{k^{-}_{0,1}}+\frac{k^{-}_{\underline{1},1}}{k^{-i}_{\underline{1},1}}\left(\frac{1}{k^{+}_{1,1}}+\frac{1}{k^{-}_{1,1}}\right)$$

$$= \frac{1}{k^{-}_{1,1}}+\frac{1}{k^{+}_{1,0}}+\frac{k^{+}_{1,1}}{k^{-o}_{1,\underline{1}}}\left(\frac{1}{k^{+}_{1,1}}+\frac{1}{k^{-}_{1,1}}\right) \simeq \frac{1}{v^{-}_{1,\underline{1}}}$$

$$\simeq \frac{1}{18.3 \text{ } \mu\text{mol/min per g wet cells}} \qquad (18c)$$

$$\frac{1}{v^{+}_{1,\underline{1}}} \simeq \frac{1}{k^{+}_{1,1}}+\frac{1}{k^{-}_{1,0}}+\frac{k^{-}_{1,1}}{k^{-i}_{1,\underline{1}}}\left(\frac{1}{k^{+}_{1,1}}+\frac{1}{k^{-}_{1,1}}\right)$$

$$= \frac{1}{k^{-}_{1,1}}+\frac{1}{k^{+}_{0,1}}+\frac{k^{+}_{1,1}}{k^{-o}_{\underline{1},1}}\left(\frac{1}{k^{+}_{1,1}}+\frac{1}{k^{-}_{1,1}}\right) \simeq \frac{1}{v^{-}_{\underline{1},1}}$$

$$\simeq \frac{1}{33.1 \text{ } \mu\text{mol/min per g wet cells}} \qquad (18d)$$

in which lactose transport mediated by either site m or μ in the doubly-occupied m : μ dimer now displays comparatively low affinity (Eqns. 18a and 18b) even though the binding of lactose to site m^{B}_{i} or μ^{B}_{o} is intrinsically of high affinity (Eqn. 13h), again due to partially rate-determining galactoside-H^{+} dissociation/-$^{-}$OH binding.

The K_m and V_{max} values predicted by Eqns. 15 and 17 may be compared with the experimental values obtained for lactose transport in non-energized ML308-225 cells [21] and membrane vesicles [30,34,35]. For this purpose, the V_{max} values reported for the latter system (in units of nmol/min per mg membrane protein) [34,35] must be divided by a factor of 3.0 for comparison with values reported for intact cells (expressed as μmol/min per g wet cells) [21]; using this conversion factor, both intact cells and vesicles yield identical maximum velocities for high-affinity lactose uptake under energized conditions of 36–40 units [21,35]. From Eqns. 15 and 17, lactose transport in non-energized systems under zero-trans conditions would be predicted to exhibit a high-affinity K_m of approx. 0.9 mM (Eqn. 15a) and a V_{max} around 19–26 units (Eqns. 15b and 17b), while the experimental values for these parameters are 0.9–1.2 mM (Table I) and 19 units (reported for high-affinity lactose efflux via facilitated diffusion, Fig. 8A in Ref. 35). Under zero-trans conditions, the low-affinity transport K_m (Eqn. 17a) would normally be obscured by the high-affinity component (Eqn. 15a) because of the similarity in V_{max} values for the two processes (Eqns. 15b and 17b), although reports of low-affinity lactose efflux in CCCP-treated membrane vesicles [34,35] indicate that the low-affinity component may be observable under some conditions. On the other hand, low-affinity lactose binding is readily demonstrable in *N*-ethylmaleimide protection studies [30] and from the ability of lactose at high concentration to displace bound α-PNPG or dansylated galactosides from site m^{A}_{o} or μ^{A}_{i} [30,33].

In the presence of high levels of unlabeled lactose in the trans compartment, the velocity curve predicted for [^{14}C]lactose transport would be altered markedly from that observed under zero-trans conditions, due to the relatively high values postulated for $k^{+}_{1,1}$ and $k^{-}_{1,1}$ (Eqn. 13d). Thus, a plot of initial rates of [^{14}C]lactose transport against [^{14}C]lactose concentration under infinite-trans conditions in non-energized systems is predicted to be biphasic, manifesting a high-affinity counterflow component ($K_m \sim 1$ mM, $V_{max} \sim 15$–30 units) (Lombardi, F.J., unpublished data) and a second, low-affinity component with a K_m of approximately 20 mM and a maximum velocity, V^{x}, of

$$\frac{1}{V^{x}} < \left(\frac{1}{k^{+}_{1,1}}+\frac{1}{k^{-}_{1,1}}\right)\left(1+\frac{k^{+}_{1,1}}{k^{-o}_{\underline{1},1}}+\frac{k^{-}_{1,1}}{k^{-i\ddot{e}}_{1,\underline{1}}}\right)$$

or

$$V^{x} > 143 \text{ } \mu\text{mol/min per g wet cells} \qquad (19)$$

in accord with the very rapid exchange diffusion ob-

served in ML308-225 membrane vesicles under these conditions (Ob. 3c) [34].

To summarize this section, the kinetic picture that emerges from Eqn. 13 and Fig. 1B for interaction of external lactose with the m : μ dimer in non-energized systems consists of a high-affinity binding to the μ_o^B site ($K_{0,1}^o \simeq 0.235$ mM, Eqn. 13f) accompanied by a 25-fold reduction in the intrinsic translocation rate relative to the unoccupied dimer (Eqns. 13a and 13c) or, alternatively, low-affinity binding to the m_o^A site ($K_{1,0}^o \simeq 10$ mM, Eqn. 13e) accompanied by a small increase in the intrinsic translocation rate (Eqn. 13b). Because of the postulated rate-limiting dissociation of the transported lactose-$H^+/^-OH$ couple in the latter alternative, however, lactose transport mediated by the singly-occupied m : μ dimer would manifest a high affinity for lactose regardless of which site the sugar occupies during the transport cycle. Similarly, binding of a second molecule of lactose to the singly-occupied porter would again proceed with high affinity at site μ_o^B and with comparatively low affinity at site m_o^A, but net lactose transport mediated by the doubly-occupied m : μ dimer would exhibit low affinity for lactose regardless of which site the transported sugar vacates during the catalytic cycle, again due to rate-limiting dissociation at step $k_{1,1}^{-i}$ (Eqn. 13h). This slow dissociation step would also be responsible for the fact that the maximum velocity for low-affinity lactose transport under zero-*trans* conditions is only marginally faster than that for high-affinity transport (Eqns. 15b and 17b), whereas with high concentrations of lactose present on both sides of the membrane ($\geqslant$10 mM) this step would be bypassed in the exchange mode (Fig. 1B) thereby allowing very rapid low-affinity exchange diffusion of lactose under these conditions (Eqn. 19). It is apparent, therefore, that interactions between sites m and μ in the present model are envisioned as affecting primarily the translocation rate constants, and only minor effects are attributed to changes in binding affinity. Finally, the behavior of Class G^b galactosides other than lactose is expected to be qualitatively similar to that described above (Table I), whereas Class G^a galactosides are predicted to manifest high-affinity and low-affinity binding components at State A and B sites, respectively (Table I), though thiodigalactoside may be somewhat exceptional in possessing an intermediate affinity for the State B site [24].

Extension to systems bearing a substantial transmembrane $\Delta\tilde{\mu}_{H^+}$

The coupling of lactose transport to H^+-symport/$^-$OH-antiport in the half-sites model assures that the m : μ dimer would be thermodynamically competent to carry out concentrative uptake of both Class G^a and G^b galactosides in the presence of a transmembrane $\Delta\tilde{\mu}_{H^+}$, for which the accumulation ratio of galactoside G^n at thermodynamic equilibrium (assuming no m : μ -independent leak pathways) is

$$\left[\frac{(G^n)_i}{(G^n)_o}\right]_{eq} = K_{eq} = \exp\{-n(F/RT)\,\Delta\tilde{\mu}_{H^+}\}$$

$$= \exp\{-n[(F/RT)\,\Delta\psi - 2.3\,\Delta\,pH]\} \quad (20)$$

(cf. Eqn. 14) where n, the galactoside : $H^+/^-OH$ stoichiometry, is assumed to be the same for all galactosides (but see Ref. [69]) and to be near 1.0 [9,48]. On the other hand, the m : μ dimer would not seem to be well suited kinetically to active galactoside accumulation, due to the high affinity of sites m_i^B and μ_i^A for internal Class G^b and G^a substrates, respectively, as well as the probable negative values for $N_{1,0}$ and $N_{0,1}$ associated with net electric charge transport during inward translocation of the singly-occupied m : μ dimers (Eqn. 7b) which would favor outward rather than inward translocation of such singly occupied species in the presence of a negative $\Delta\psi$. Although the various binding and translocation constants in Fig. 1 and Eqn. 13 would be expected to vary with changes in $\Delta\psi$, pH_i and pH_o (and thus with ΔpH) subject to the conditions given in Eqns. 14 and 20, it seems unlikely that gradual changes in these constants with variation in $\Delta\tilde{\mu}_{H^+}$ could alone be responsible for the profoundly altered properties exhibited by the transporter in highly energized systems (Ob. 4a–h). These changes are readily accounted for, however, by postulating a $\Delta\tilde{\mu}_{H^+}$-induced modification of the m : μ dimer analogous in some respects to voltage-induced changes in the sodium channel of nerve cell membranes [41] resulting in a new form designated *(m : μ) whose binding and translocation properties are distinctly different from those of form m : μ. Because the limited experimental data available at the present time do not allow a unique specification of the kinetic properties of form *(m : μ), four alternative binding and trans-

location schemes are outlined below. Whatever the detailed kinetic scheme, however, extension of the half-sites model to highly energized systems entails the following postulates in addition to Po. 1–5 described above.

Po. 6. The form of the functional dimer that predominates near $\Delta\psi = \Delta pH = 0$ (i.e., form m : μ) is assumed to undergo facile interconversion with two other forms by way of an electrogenic protein conformational change,

$$\eta H_o^+ + (m : \mu)^* \leftrightarrow m : \mu \leftrightarrow {}^*(m : \mu) + \eta H_i^+ \qquad (21)$$

where η is not necessarily an integer, and where a positive $\Delta\psi$ shifts the above reaction to the left while a negative $\Delta\psi$ causes a shift to the right. Thus, in the

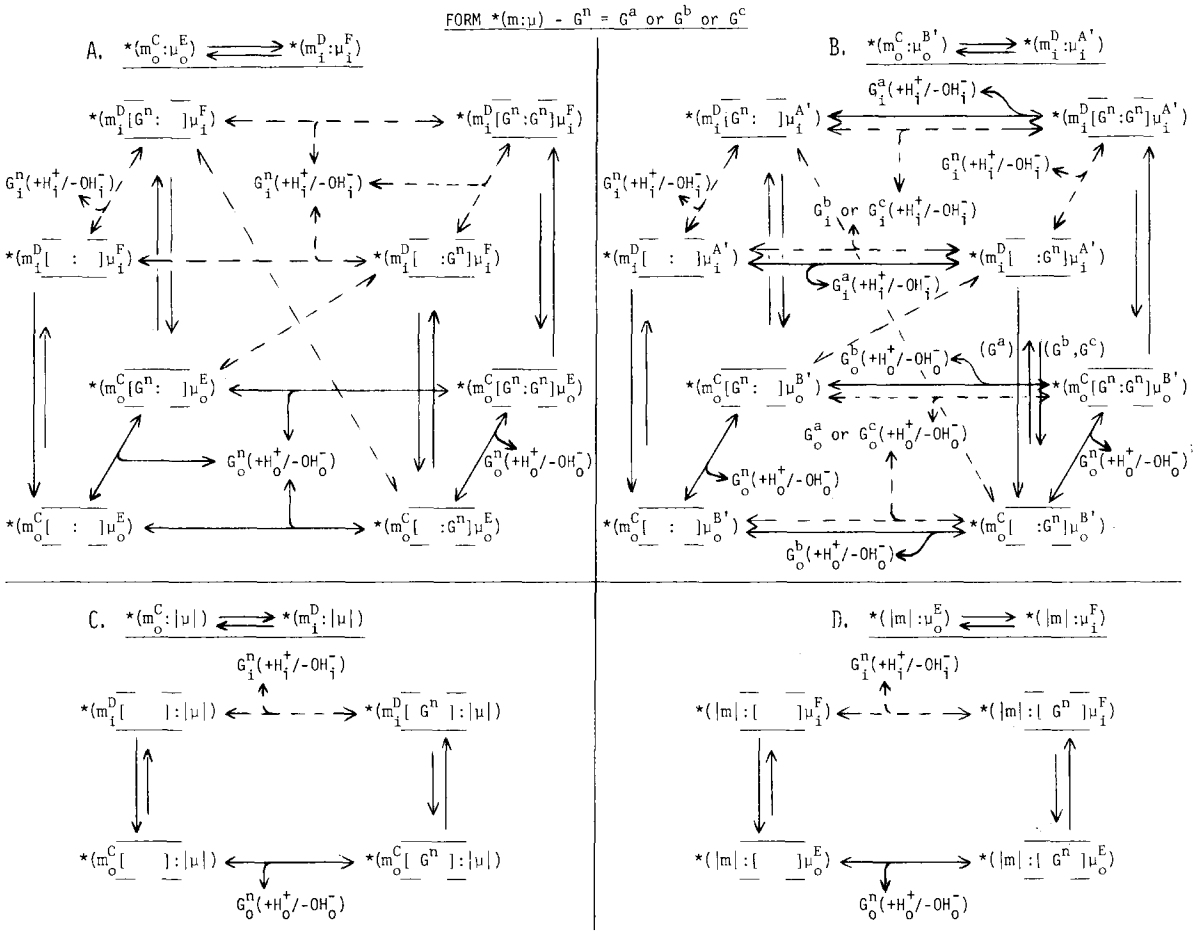

Fig. 2. Four altenative binding and translocation schemes consonant with the half-sites model for transport mediated by the *(m : μ) dimer (Eqn. 20) in membrane structures of native orientation bearing a substantial (negative) $\Delta\tilde{\mu}_{H^+}$. As in Fig. 1, solid and dashed branching arrows designate intrinsically high-affinity and intrinsically low-affinity binding, respectively, of a galactoside of the indicated Class together with binding of one H^+ or dissociation of one ^-OH ion; pairs of vartical arrows represent translocations. Other symbols are as defined in Fig. 1 and the text, except that the symbols depicting the thiodigalactoside-protectable thiol group (Fig. 1) are omitted in this representation. The postulated $\Delta\tilde{\mu}_{H^+}$-induced m : $\mu \rightarrow$ *(m : μ) transition (see Eqn. 20) brings about changes in one or both binding sites such that a high affinity for external Class G^a, G^b and G^c galactosides together with a low affinity toward internal Class G^a, G^b and G^c galactosides is exhibited by: A, both the m and the μ binding sites; B and C, the m binding site alone; or D, the μ binding site alone. In alternative B, the μ binding site remains essentially unchanged relative to its properties in form m : μ. In variant C, the μ binding site has been inactivated by the m : $\mu \rightarrow$ *(m : μ) transition (i.e., |μ|), while in version D this transition inactivates binding site m (i.e., |m|).

presence of a $\Delta\tilde{\mu}_{H^+}$ of normal (negative) polarity, the transporter is assumed to undergo a $\Delta\psi$- and/or ΔpH-induced hysteresis between forms m : μ and *(m : μ). The midpoint potential at which forms m : μ and *(m : μ) would be present in equal concentration ($\Delta^{\star}\tilde{\mu}_{H^+}$) is difficult to estimate from available data, but may lie in the range −30 to −60 mV [36] or more.

Po. 7. In form *(m : μ), either the m or the μ binding site (or both) would be altered to assume new States in one of at least four alternative patterns consistent with Ob. 4a–h.

(a) With the outer gate (g_o) open and the inner gate (g_i) closed, both sites m and μ might be modified into functionally similar but distinct States (m_o^C and μ_o^E) possessing high affinity toward both Class G^a and G^b galactosides (Table I) as well as additional galactosides such as APG_0 and APG_2 which are bound poorly in States A and B [43,44] and are therefore designated Class G^c galactosides (Table I); with g_o closed and g_i open, on the other hand, sites m and μ would adopt States (m_i^D and μ_i^F) displaying low affinity for all galactosides (Fig. 2A).

(b) Alternatively, binding site m in form *(m : μ) might adopt States m_o^C and m_i^D as defined above, while binding site μ would remain essentially unchanged relative to its behavior in form m : μ, manifesting States $\mu_o^{B'}$ and $\mu_i^{A'}$ (Fig. 2B); the complementary pattern in which site μ would be altered but site m would remain essentially unchanged in form *(m : μ) is ruled out by the observation that lactose at low concentrations protects against *N*-ethylmaleimide inactivation in highly energized systems (Ob. 4c).

(c) In the third alternative, binding site m might adopt States m_o^C and m_i^D as defined above, whereas site μ would be rendered nonfunctional in form *(m : μ) (i.e., |μ| in Fig. 2C).

(d) Finally, binding site μ might adopt States μ_o^E and μ_i^F as defined above (Table I), while site m would be nonfunctional in form *(m : μ) (i.e., |m| in Fig. 2D).

Po. 8. In form *(m : μ), translocation of a galactoside bound to either site m or μ is again presumed to require protonation of an associated -X subsite (Eqns. 3–6) (or, alternatively, dissociation of $^{-}$OH from its subsite), leading to a galactoside-$H^+/^{-}$OH transport stoichiometry near 1.0 [12]. Absorbing the explicit -X notation as before into the adjacent symbols and representing translocation by the implicit symbolism of Eqns. 8–11 (except for suppression of the -SH, HS- notation as explained below), then translocation of the unoccupied *(m : μ) dimer in the four alternative schemes of Fig. 2 may be written

$$^{\star}(m_o^{C}\overline{[\ :\ ]}\,\mu_o^{E}) \rightleftharpoons {}^{\star}(m_i^{D}\underline{[\ :\ ]}\,\mu_i^{F}), \quad {}^{\star}N_{0,0} < 0 \tag{22a}$$

$$^{\star}(m_o^{C}\overline{[\ :\ ]}\,\mu_o^{B'}) \rightleftharpoons {}^{\star}(m_i^{D}\underline{[\ :\ ]}\,\mu_i^{A'}), \quad {}^{\star}N_{0,0} < 0 \tag{22b}$$

$$^{\star}(m_o^{C}\overline{[\ ]}:\overline{|\mu|}) \rightleftharpoons {}^{\star}(m_i^{D}\underline{[\ ]}:\underline{|\mu|}), \quad {}^{\star}N_{0,0} < 0 \tag{22c}$$

$$^{\star}(\overline{|m|}:\overline{[\ ]}\,\mu_o^{E}) \rightleftharpoons {}^{\star}(\underline{|m|}:\underline{[\ ]}\,\mu_i^{F}), \quad {}^{\star}N_{0,0} < 0 \tag{22d}$$

where [ ] represents the pore within the *(m : μ) dimer, upper and lower horizontal bars depict the inner gate (g_i) and the outer gate (g_o), respectively, and the $^{\star}N_{0,0}$ is the effective inward charge transport (not necessarily an integer) associated with inward translocation of the *(m : μ) dimer. Similarly, translocation in the singly occupied *(m : μ) dimer may be represented by

$$^{\star}(m_o^{C}\overline{[G\ :\ ]}\,\mu_o^{E}) \rightleftharpoons {}^{\star}(m_i^{D}\underline{[G\ :\ ]}\,\mu_i^{F}), \quad {}^{\star}N_{1,0} \simeq 0$$

$$^{\star}(m_o^{C}\overline{[\ :\ G]}\,\mu_o^{E}) \rightleftharpoons {}^{\star}(m_i^{D}\underline{[\ :\ G]}\,\mu_i^{F}), \quad {}^{\star}N_{0,1} \simeq 0 \tag{23a}$$

$$^{\star}(m_o^{C}\overline{[G\ :\ ]}\,\mu_o^{B'}) \rightleftharpoons {}^{\star}(m_i^{D}\underline{[G\ :\ ]}\,\mu_i^{A'}), \quad {}^{\star}N_{1,0} \simeq 0$$

$$^{\star}(m_o^{C}\overline{[\ :\ G]}\,\mu_o^{B'}) \rightleftharpoons {}^{\star}(m_i^{D}\underline{[\ :\ G]}\,\mu_i^{A'}), \quad {}^{\star}N_{0,1} \simeq 0 \tag{23b}$$

$$^{\star}(m_o^{C}\overline{[G]}:\overline{|\mu|}) \rightleftharpoons {}^{\star}(m_i^{D}\underline{[G]}:\underline{|\mu|}), \quad {}^{\star}N_{1,0} > 0 \tag{23c}$$

$$^{\star}(\overline{|m|}:\overline{[G]}\,\mu_o^{E}) \rightleftharpoons {}^{\star}(\underline{|m|}:\underline{[G]}\,\mu_i^{F}), \quad {}^{\star}N_{0,1} > 0 \tag{23d}$$

and translocation in the doubly occupied dimer by

$$^{\star}(m_o^{C}\overline{[G:G]}\,\mu_o^{E}) \rightleftharpoons {}^{\star}(m_i^{D}\underline{[G:G]}\,\mu_i^{F}), \quad {}^{\star}N_{1,1} > 0\,; \tag{24a}$$

$$^{\star}(m_o^{C}\overline{[G:G]}\,\mu_o^{B'}) \rightleftharpoons {}^{\star}(m_i^{D}\underline{[G:G]}\,\mu_i^{A'}), \quad {}^{\star}N_{1,1} > 0\,; \tag{24b}$$

where G represents a galactoside molecule, and the $^{\star}N_{j,k}$ again denote the effective charges translocated inward in association with translocation of the corresponding species (reading from left to right).

Po. 9. Apart from the observation that low concentrations of lactose as well as thiodigalactoside protect against *N*-ethylmaleimide inactivation in energized systems [51], the available experimental data do not seem to allow the characteristics of the protectable thiol group in form $^{\star}(m : \mu)$ to be defined in a diagnostically useful manner. Accordingly, the detailed properties of this thiol in form $^{\star}(m : \mu)$ are left unspecified at this time.

Kinetic properties ($\Delta\tilde{\mu}_{H^+} << 0$)

As indicated above, the four alternative binding and translocation schemes for form $^{\star}(m : \mu)$ in Fig. 2 are all consonant with the half-sites concept, and all are compatible with the experimental results when $\Delta\tilde{\mu}_{H^+} << 0$ (Ob. 4a–h). Thus, the four schemes all exhibit high affinity toward external lactose but low affinity for internal lactose (Ob. 4a, b), mutual competition among galactosides of Classes G^a, G^b and G^c for high-affinity binding and uptake (Ob. 4c, d, g), and exchange rates similar to net rates of uptake or efflux (Ob. 4e). Moreover, the widely varying maximum velocities for uptake observed with different galactosides (Ob. 4f) are readily incorporated into the schemes in Fig. 2. Finally, by assuming that outward translocation of a bound galactoside may occasionally occur with the associated -X group unprotonated (Eqns. 4–6) (or, alternatively, with a corresponding $^{-}$OH group undissociated) in site m or μ of form $^{\star}(m : \mu)$, a simple explanation is provided for the apparent transporter mediated galactoside leak pathway (Ob. 4h). Pronounced enhancement of such leak pathways is presumably responsible for the properties of the accumulation-deficient (uncoupled) mutants ML308-22 and K12 X71-54 described by West and Wilson [70].

The four alternative kinetic schemes for the $^{\star}(m : \mu)$ dimer in Fig. 2 are probably readily distinguishable on the basis of binding, transport, and *N*-ethylmaleimide-inactivation studies. Thus, experiments using a broad range of Class G^a, G^b and G^c galactosides in energized systems would be predicted by the schemes in Fig. 2A and Fig. 2B to uncover some substrate pairs displaying incomplete or negligible competition for high-affinity uptake, whereas the mechanisms in Fig. 2C and Fig. 2D would predict essentially complete competitive inhibition. The nature of the inhibition observed with various substrate pairs needs to be carefully established in order to distinguish competition for binding from possible non-competitive effects occasioned by the low maximum velocity of transport for certain galactosides (Ob. 4f). Furthermore, the schemes in both Fig. 1A and Fig. 1B predict rapid accumulation of Class G^b galactosides, but only the former is consistent with rapid accumulation of Class G^a transport substrates, since the high affinity of site $\mu_i^{A'}$ for internal Class G^a galactosides in the latter mechanism would cause significant transporter-mediated efflux of these substrates, thereby producing a major kinetic reversal of the uptake flow via the m site.

Specific predictions of the half-sites model

As well as satisfying the observational requirements listed in Ob. 1–4, the half-sites model specifies the following unique predictions.

Pr. 1. The model predicts half-sites stoichiometry for high-affinity binding of α-PNPG, thiodigalactoside and dansylated galactosides in non-energized systems [27,30,33,45–47].

Pr. 2. The model suggests half-sites stoichiometry for rapid reaction of the protectable thiol group with *N*-ethylmaleimide under non-energized conditions.

Pr. 3. The model predicts two topologically distinct locations of the protectable thiol, as reported by Yariv et al. [71].

Pr. 4. Under non-energized conditions, the transporter is predicted to mediate high-affinity facilitated diffusion of Class G^a galactosides such as α-PNPG and thiodigalactoside in a manner not susceptible to inhibition by lactose at concentrations below 5 mM [3,25].

Pr. 5. The model predicts that the very rapid low-affinity exchange diffusion observed in non-energized systems when lactose is present at $\geqslant$10 mM concentration on both sides of the membrane [34] will be found to be inhibited by low concentrations ($<$50 μM) of the Class G^a galactoside α-PNPG, due to binding of the latter at the State A site and consequent slowing of the translocation rate (Figs. 1A and 1B, Eqn. 13).

It should be noted that reports have recently appeared suggesting possible interactions of the galactoside transporter with *E. coli* β-galactoside [72,73]. Accordingly, experiments aimed at testing models for

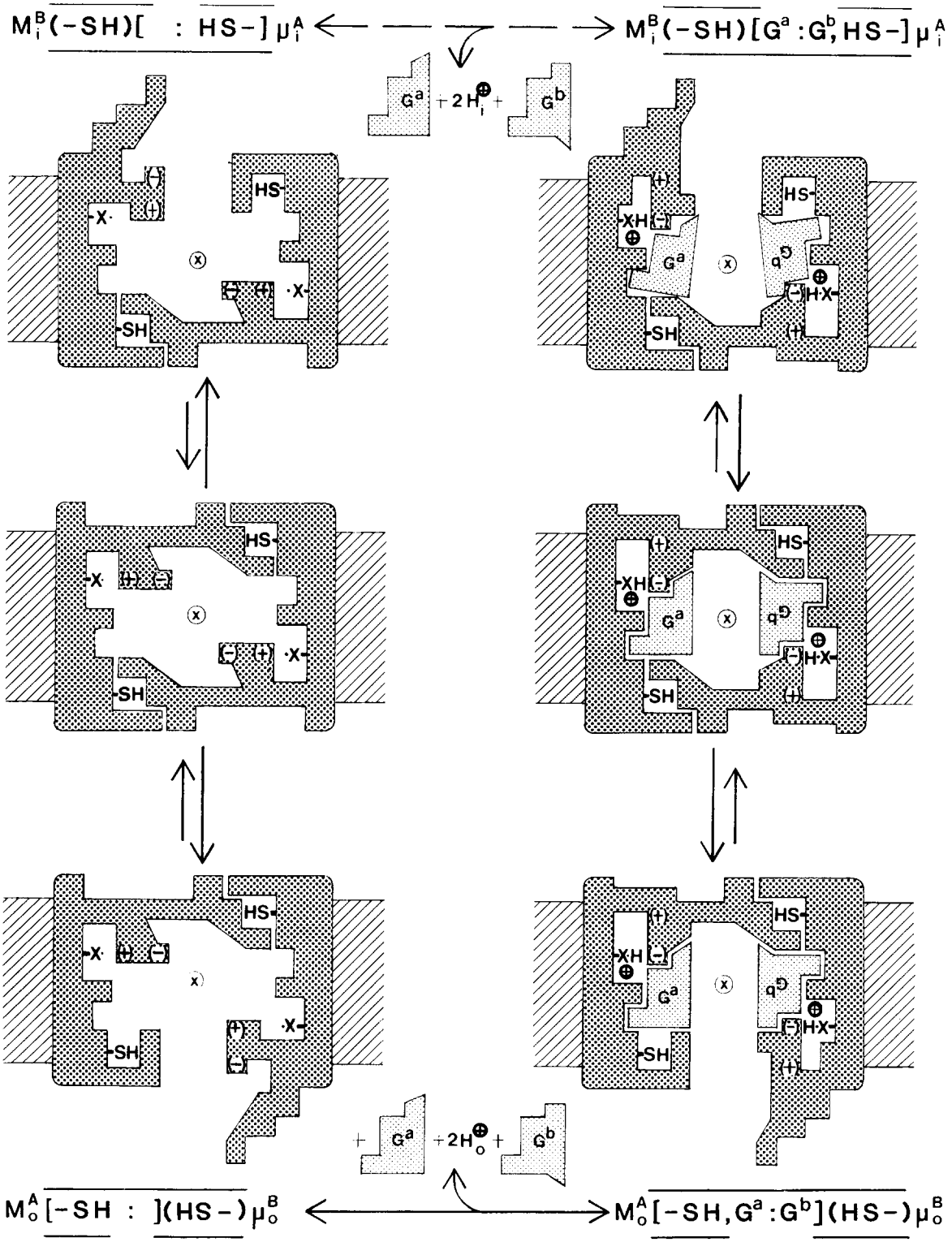
M_i^B(-SH)[: HS-]μ_i^A
M_i^B(-SH)[G^a : G^b, HS-]μ_i^A
G^a + 2H_i^⊕ + G^b
HS
SH
X
XH
H·X
G^a
G^b
M_o^A[-SH :](HS-)μ_o^B
M_o^A[-SH, G^a : G^b](HS-)μ_o^B
G^a + 2H_o^⊕ + G^b

the transporter using intact cells would be most easily interpretable with strains lacking the β-galactosidase protein.

Discussion

Fig. 3 illustrates in a speculative pictorial fashion the basic principles of the half-sites model governing binding and translocation in the postulated m : μ functional dimer. As shown (Fig. 3, bottom), high-affinity binding of a Class G^a galactoside (plus H^+) to site m_o^A together with high-affinity binding of a Class G^b galactoside (plus H^+) to site μ_o^B may be followed by closing of the outer gate to form the transition state for translocation (Fig. 3, right center). Subsequent opening of the inner gate and accompanying shifts in the binding States to m_i^A and μ_i^B would greatly enhance dissociation of the transported galactosides and H^+ ions (assuming no trans-site migration during translocation) (Fig. 3, top). Finally, return of the unoccupied binding sites to the exterior without concomitant H^+ transport is ensured by appropriate juxta-position of the postulated H^+-carrying subsites (-X•) with charged groups of the inner and outer gates in the symmetrical transition state for translocation (Fig. 3, left center). Similar considerations would govern interaction of Class G^a, G^b and G^c galactosides with the form of the transporter postulated to predominate under highly energized conditions, i.e., *(m : μ) (not shown).

The galactoside transporter of *E. coli* is the only uptake system for which a symmetrical half-sites model has been suggested to date. However, the advantages of such a structure for systems of broad substrate specificity would seem to be manifold, offering the potential for two related transport systems at the genetic cost of one. Moreover, recent results on the integration of proteins into biological membranes [74] suggest that dimerization of newly synthesized *lac*Y protein prior to incorporation into the membrane would represent a reasonable sequence of events.

The evolutionary implications of the half-sites interpretation for the galactoside transporter are particularly interesting. It may be presumed that the system originated as a symmetrical dimer mediating facilitated diffusion of some β-galactosides via two independent channels each containing a single binding site. Subsequent interaction and fusion of the two channels into a single gated pore would have created two distinct galactoside binding sites per dimer, thereby allowing expansion of the range of transportable substrates to include some α- as well as additional β-galactosides. However, utilization of this broad range of substrates as carbon and energy sources requires hydrolysis by intracellular α- and β-galactosidases, but the affinity of these enzymes for some of the transported substrates would have been low, thus providing a selective pressure for increasing the intracellular galactoside concentration. Coupling of galactoside transport to H^+-symport/$^-$OH-antiport was presumably adopted in response to this pressure, and would probably have been followed by development of the m : $\mu \rightarrow {}^\star$(m : μ) transition for decreasing the affinity of the transport system toward internal Class G^b galactosides. Finally, the employment by *E. coli* of allolactose and galactobiose, produced by the transgalactosidase activity of β-galactosidase, as natural inducers of the *lac* operon [75] may have been a later evolutionary development to reduce the frequency of gratuitous induction due to accumulation [76] of naturally occurring unhydrolyzable galactosides.

Conclusion

Verification of the half-sites model for the *E. coli* galactoside transporter will require confirmation of Predictions 1–5 as well as further structural work including radiation inactivation studies [77]. It is hoped that the recent development of techniques for solubilization and reconstitution of specific transport activity in liposomes [63] will allow a definitive test of the half-sites model in the near future.

Fig. 3. Speculative depiction of binding and translocation postulated by the half-sites model for the *E. coli* galactoside transporter as mediated by the m : μ functional dimer (Eqn. 20) in the presence of a Class G^a galactoside (e.g., melibiose) and a Class G^b galactoside (e.g., lactose). The symbols -X• denote H^+-symporting groups (Eqns. 3–6); ○ designates the 2-fold axis of rotational symmetry present in the transition state for translocation in the unoccupied dimer (left center). Other symbols are as defined in Fig. 1 and the text (Discussion).

Acknowledgements

I thank Drs. J.F. Mead and A.J. Fulco for their aid during the course of this work.

References

1 Cohen, G.N. and Rickenberg, H.V. (1955) Compt. Rend. 240, 466–468
2 Rickenberg, H.V., Cohen, G.N., Buttin, G. and Monod, J. (1956) Ann. Inst. Past. 91, 829–857
3 Kennedy, E.P. (1970) in The Lactose Operon (Beckwith, J.R. and Zipser, D., eds.), pp. 49–92, Cold Spring Harbor Laboratory Press, Cold Spring Harbor, New York
4 Harold, F.M. (1977) Curr. Top. Bioenerg. 6, 83–149
5 Wilson, D.B. (1978) Annu. Rev. Biochem. 47, 933–965
6 West, I.C. (1980) Biochim. Biophys. Acta 604, 91–126
7 Mitchell, P. (1963) Biochem. Soc. Symp. 22, 142–168
8 West, I.C. (1970) Biochem. Biophys. Res. Commun. 41, 655–661
9 West, I.C. and Mitchell, P. (1973) Biochem. J. 132, 587–592
10 Hirata, H., Altendorf, K. and Harold, F.M. (1973) Proc. Natl. Acad. Sci. U.S.A. 70, 1804–1808
11 Cecchini, G. and Koch, A.L. (1975) J. Bacteriol. 123, 187–195
12 Purdy, D.R. and Koch, A.L. (1976) J. Bacteriol. 127, 1188–1196
13 Flagg, J.L. and Wilson, T.H. (1978) Membrane Biochem. 1, 61–72
14 Fox, C.F. and Kennedy, E.P. (1965) Proc. Natl. Acad. Sci. U.S.A. 54, 891–899
15 Fox, C.F., Carter, J.R. and Kennedy, E.P. (1967) Proc. Natl. Acad. Sci. U.S.A. 57, 698–705
16 Jones, T.H.D. and Kennedy, E.P. (1969) J. Biol. Chem. 244, 5981–5987
17 Büchel, D.E., Gronenborn, B. and Müller-Hill, B. (1980) Nature 283, 541–545
18 Villarejo, M. (1980) Biochem. Biophys. Res. Commun. 93, 16–23
19 Ehring, R., Beyreuther, K., Wright, J.K. and Overath, P. (1980) Nature 283, 537–540
20 Chang, C.N., Blobel, G. and Model, P. (1978) Proc. Natl. Acad. Sci. U.S.A. 75, 361–365
21 Winkler, H.H. and Wilson, T.H. (1966) J. Biol. Chem. 241, 2200–2211
22 Lancaster, J.R., Hill, R.J. and Struve, W.G. (1975) Biochim. Biophys. Acta 401, 285–298
23 Teather, R.M., Haemlin, O., Schwarz, H. and Overath, P. (1977) Biochim. Biophys. Acta 467, 386–395
24 Lancaster, J.R., Jr. and Hinkle, P.C. (1977) J. Biol. Chem. 252, 7657–7661
25 Lancaster, J.R., Jr. and Hinkle. P.C. (1977) J. Biol. Chem. 252, 7662–7666
26 Pavlasova, E. and Harold, F.M. (1969) J. Bacteriol. 98, 198–204
27 Kennedy, E.P., Rumley, M.K. and Armstrong, J.B. (1974) J. Biol. Chem. 249, 33–37
28 Hsu, C.C. and Fox, C.F. (1970) J. Bacteriol. 103, 410–416
29 Kepes, A. (1960) Biochim. Biophys. Acta 40, 70–84
30 Wright, J.K., Teather, R.M. and Overath, P. (1979) in Function and Molecular Aspects of Biomembrane Transport (Klingenberg, E.M., Palmieri, F. and Quagliariello, E., eds.), pp. 239–248, Elsevier/North Holland, Amsterdam
31 Hobson, A.C., Gho, D. and Müller-Hill, B. (1977) J. Bacteriol. 131, 830–838
32 Langridge, J. (1974) Aust. J. Biol. Sci. 27, 331–340
33 Schuldiner, S. and Kaback, H.R. (1977) Biochim. Biophys. Acta 472, 399–418
34 Kaczorowski, G.J. and Kaback, H.R. (1979) Biochemistry 18, 3691–3697
35 Kaczorowski, G.J., Robertson, D.E. and Kaback, H.R. (1979) Biochemistry 18, 3697–3704
36 Robertson, D.E., Kaczorowski, G.J., Garcia, M.-L. and Kaback, H.R. (1980) Biochemistry 19, 5692–5702
37 Lancaster, J.R. (1978) J. Theor. Biol. 75, 35–50
38 Singer, S.J. (1977) J. Supramol. Struc. 6, 313–323
39 Baker, G.F. and Widdas, W.F. (1973) J. Physiol. (London) 231, 129–142
40 Barnett, J.E., Holman, G.D., Chalkley, R.A. and Munday, K.A. (1975) Biochem. J. 145, 417–429
41 Keynes, R.D. and Rojas, E. (1974) J. Physiol. (London) 239, 393–434
42 Lombardi, F.J. (1980) Fed. Proc. 39, 2158
43 Rudnick, G., Weil, R. and Kaback, H.R. (1975) J. Biol. Chem. 250, 1371–1375
44 Rudnick, G., Weil, R. and Kaback, H.R. (1975) J. Biol. Chem. 250, 6847–6851
45 Overath, P., Teather, R.M., Simoni, R.D., Aichele, G. and Wilhelm, U. (1979) Biochemistry 18, 1–11
46 Belaich, A., Simonpietri, P. and Belaich, J.-P. (1976) J. Biol. Chem. 251, 6735–6738
47 Toci, R., Belaich, A. and Belaich, J.-P. (1980) J. Biol. Chem. 255, 4603–4606
48 Zilberstein, D., Schuldiner, S. and Padan, E. (1979) Biochemistry 18, 669–673
49 Kaback, H.R. and Barnes, E.M., Jr. (1971) J. Biol. Chem. 246, 5523–5531
50 Putzrath, R.M. and Wilson, T.H. (1979) J. Bacteriol. 137, 1037–1039
51 Kepes, A. (1970) in Current Topics in Membranes and Transport (Bonner, F. and Kleinzeller, A., eds.), Vol. I, pp. 101–134, Academic Press, London
52 Rudnick, G., Schuldiner, S. and Kaback, H.R. (1976) Biochemistry 15, 5126–5131
53 Kaczorowski, G.J., LeBlanc, G. and Kaback, H.R. (1980) Proc. Natl. Acad. Sci. U.S.A. 77, 6319–6323
54 Booth, I.R., Mitchell, W.J. and Hamilton, W.A. (1979) Biochem. J. 182, 687–696
55 Booth, I.R. (1980) Biochem. Soc. Trans. 8, 276–278
56 Booth, I.R. and Hamilton, W.A. (1980) Biochem. J. 188, 467–473

57 Feile, H., Porter, J.S., Slayman, C.L. and Kaback, H.R. (1980) Biochemistry 19, 3585–3590
58 Ramos, S., Schuldiner, S. and Kaback, H.R. (1976) Proc. Natl. Acad. Sci. U.S.A. 73, 1892–1896
59 Ramos, S. and Kaback, H.R. (1977) Biochemistry 16, 848–853
60 Ramos, S. and Kaback, H.R. (1977) Biochemistry 16, 854–859
61 Carter, J.R., Fox, C.F. and Kennedy, E.P. (1968) Proc. Natl. Acad. Sci. U.S.A. 60, 725–732
62 Barnes, E.M. and Kaback, H.R. (1970) Proc. Natl. Acad. Sci. U.S.A. 66, 1190–1198
63 Newman, M.J. and Wilson, T.H. (1980) J. Biol. Chem. 255, 10583–10586
64 Hertzberg, E.L. and Hinkle, P.C. (1974) Biochem. Biophys. Res. Commun. 58, 178–184
65 Mitchell, P. (1976) Biochem. Soc. Trans. 4, 399–430
66 Turner, R.J. and Silverman, M. (1980) Biochim. Biophys. Acta 596, 272–291
67 King, E.L. and Altman, C. (1956) J. Phys. Chem. 60, 1375–1378
68 Lieb, W.R. and Stein, W.D. (1974) Biochim. Biophys. Acta 373, 178–196
69 Maloney, P.C. and Wilson, T.H. (1978) Biochim. Biophys. Acta 511, 487–498
70 West, I.C. and Wilson, T.H. (1973) Biochem. Biophys. Res. Commun. 50, 551–558
71 Yariv, J., Kalb, A.J., Katchalski, E., Goldman, R. and Thomas, E.W. (1969) FEBS Lett. 5, 173–176
72 Huber, R.E., Pisko-Dubienski, R. and Hurlburt, K.L. (1980) Biochem. Biophys. Res. Commun. 96, 656–661
73 Villarejo, M. and Ping, C. (1978) Biochem. Biophys. Res. Commun. 82, 935–942
74 Wickner, W. (1979) Annu. Rev. Biochem. 48, 23–45
75 Jobe, A. and Bourgeois, S. (1972) J. Mol. Biol. 69, 397–408
76 Kusch, M. and Wilson, T.H. (1973) Biochim. Biophys. Acta 311, 109–122
77 Kempner, E.S., Miller, J.H., Schlegel, W. and Hearon, J.Z. (1980) J. Biol. Chem. 255, 6826–6831